MAGNETIC PROPERTIES AND DILATATION OF FeNbCuBSi ALLOYS

B. Butvinová, G. Vlasák, P. Butvin, E. Illeková
Institute of Physics, Slovak Academy of Sciences, 84228 Bratislava, Slovakia

Received 1 June 2000, in final form 29 October 2000, accepted 7 December 2000

Correlation between thermal expansion and magnetic anisotropy in FeNbCuBSi alloys with 3 and 4.5 at.% Nb with various Si contents has been investigated. Besides expected influence of Nb as a crystal-growth-hampering component, specific effect of Nb in macroscopically heterogeneous ribbons is indicated. The heterogeneity is due to chemically active surfaces of the ribbons. It emerges after air annealing and varies markedly with the contents of Si. Despite promoting thermal expansion prior to crystallization, the complex chemical reactions on air exposed surfaces result in more crystallized surfaces that squeeze the underlying volume. The evidence of squeezing comes from characteristic magnetic anisotropy.

PACS: 65.70.+y, 75.30.Gw, 75.50.Kj

1 Introduction

Excellent soft magnetic properties of nanocrystalline materials are already being exploited (e.g. in switched-mode power supplies). The material is prepared from amorphous ribbons by suitable thermal treatment to attain the optimal, partially nanocrystalline structure. Major theoretical concepts explaining the magnetic properties are based on microscopic effects as inter-grain interaction and grain size effect [1, 2]. Macroscopic properties are paid less attention although they contribute to the magnetic anisotropy too. Besides the extensively studied direct effects of chemical composition and magnetostriction, secondary influences as as-cast anelastic strain [3] and/or macroscopic heterogeneity [4, 5] are significant for the resulting magnetic properties. We try to shed more light on the role of the latter influences by investigating the correlation between thermal expansion and magnetic anisotropy in FeNbCuBSi alloys with 3 at.% Nb and 4.5 at.% Nb with various Si contents.

2 Experimental

As-cast samples were prepared by planar-flow casting on air. The straight strips for dilatation measurements were 35 mm long and 10 mm wide with thickness about 23 μm. "Dilatation" always means changing the dimension along but one of the two major axes within the ribbon plane. The samples were checked for thermal expansion up to 900 K at a rate of 7 K/min in a capacitive dilatometer [6] in Ar or air ambience. The method is capable of reproducibly resolving

$\Delta l/l$ as low as 10^{-5}. After subsequent cooling to room temperature (r.t.), the shrinkage of (then partially nanocrystallized) samples was determined as net final $\Delta l/l$. The crystallization progress and crystallization temperature T_x were determined on Perkin-Elmer DSC7 at 10 K/min heating rate to 900 K in N_2 ambience. Three-terminal capacitance method was used to obtain the coefficient of saturation magnetostriction λ_s on disk-shaped samples electrolytically etched prior to annealing. For permeability measurements, toroids with inner/outer diameter 3/3.35 cm, mass about 10 g, were wound under tensile stress 3 MPa and annealed at 540 °C for 1 h in Ar atmosphere however, without prior evacuation. The initial permeability μ_i was determined from the flat part of low-field amplitude permeability $\mu_a H$-variation according to

$$\mu_a = \frac{c_m u_a}{4\mu_0 N n S f I_p}, \tag{1}$$

where c_m is the mean magnetic path, N is the excitation windings number, n is the pick-up coil windings number, S the cross section, f the frequency (210 Hz), U_a the average value of the pick-up voltage and I_p is the peak value of magnetization current. Straight samples (vacuum and air annealed) of 10 cm length inserted in Helmholtz coils driven at 21 Hz (sine H) were used for hysteresis loops recording. Demagnetization factors were computed by numerical integration and demagnetizing field was subtracted from the external field — this is the meaning of H_i (internal field). Magnetization work W_m was computed as the mean loop intercept from 1-st and 3-rd quadrant.

3 Results and discussion

Encoding and properties of the studied materials are shown in Table 1. The asterisk should help to distinct between 3 and 4.5 at.% of Nb.

Alloy	Composition	$\lambda_s \times 10^6$	T_x [K]	$\mu_i \times 10^{-3}$	H_{cd} [A/m]	W_m [J/m^3]	B_{600} [T]
$Si_{4.5}$	$Fe_{78}Nb_3Cu_1B_{13.5}Si_{4.5}$	10.2	746	4.8	18	175	1.47
$Si_{9.2}$	$Fe_{74.8}Nb_3Cu_1B_{12}Si_{9.2}$	8	798	12	12.3	63	1.27
Si_{13}	$Fe_{73.5}Nb_3Cu_1B_{9.5}Si_{13}$	3	813	85	2.1	1.5	1.20
$Si_{13.5}$	$Fe_{73.5}Nb_3Cu_1B_9Si_{13.5}$	2.7	813	123	1.6	1.4	1.20
Si_{16}	$Fe_{73.5}Nb_3Cu_1B_{6.5}Si_{16}$	-2.8	799	27◇	3.5◇	5.8◇	1.10◇
Si_0*	$Fe_{77.5}Nb_{4.5}Cu_1B_{17.5}$	7.2	783	5◇	19.7◇	190◇	1.24◇
Si_{10}*	$Fe_{72.5}Nb_{4.5}Cu_1B_{12}Si_{10}$	8	823	22	5	15	1.23
$Si_{13.5}$*	$Fe_{72}Nb_{4.5}Cu_1B_9Si_{13.5}$	3.3	848	30	2.1	6.3	1.10
$Si_{16.2}$*	$Fe_{70.3}Nb_{4.5}Cu_1B_8Si_{16.2}$		836	34	2.4	8.8	1.11

Table 1. Properties of investigated nanocrystalline ribbons. The composition was determined by Inductionally Coupled Plasma Spectroscopy (ICPS) analysis. The temperature T_x is the temperature, at which the DSC crystallization exotherm peaks. The diamond symbol indicates straight-strip values, whereas other values in columns 5 to 8 are determined on toroids. H_{cd} is dynamic coercivity at 21 Hz. B_{600} is induction at 600 A/m.

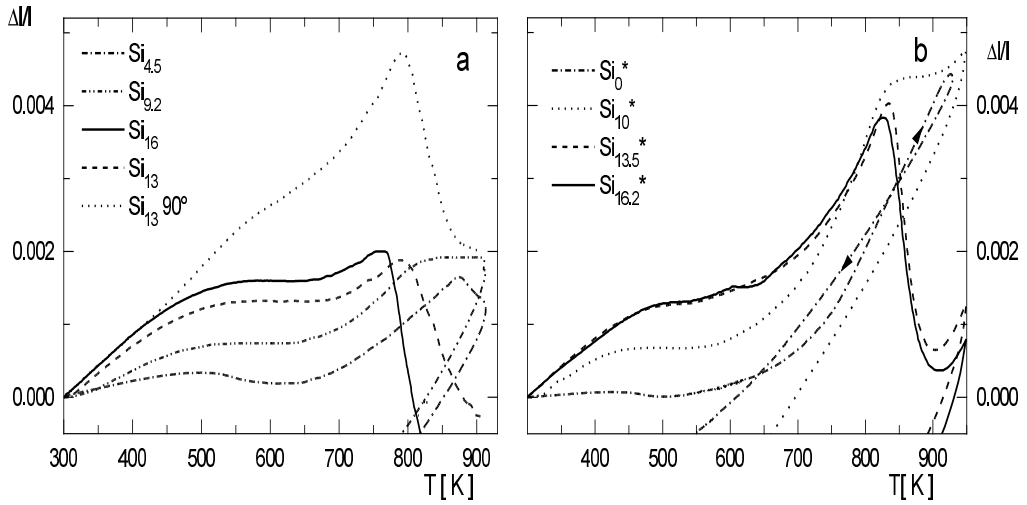

Fig. 1. Longitudinal dilatation of as-cast ribbons of Nb_3 compositions (a) and of $Nb_{4.5}$ compositions (b). Heating in Ar. Typical transverse (i.e. along the ribbon's width; symbol 90) dilatation is shown for Si_{13}.

Longitudinal dilatation curve reflects normal thermal expansion of a metal with superimposed small or larger plateau that is in general interpreted as the consequence of structural relaxation and invar effect [7,8]. However, magnitude of this effect depends also on the amount of as-cast anelastic strain introduced during the ribbon casting [3, 9]. Especially the initial part of the whole ribbon is often found without the relaxation plateau [3]; these parts have not been incorporated in experiments. Dilatation curves for different compositions of the material FeNbCuBSi are displayed in Fig. 1. Sample Si_{13} represents how $\Delta l/l$ is different when we measure the dimension changes along or transverse (i.e. along the ribbon width) to the ribbon long axis. Larger dilatation almost without relaxation plateau is observed at transversal orientation. The anisotropic $\Delta l/l$ response indicates the existence of an as-cast structural anisotropy due to the anelastic strain. This often goes with a characteristic contribution to the as-cast magnetic anisotropy [9]. The anisotropic expansion affects the net shrinkage too. This anisotropy is almost completely smeared off if the expansion and shrinkage is observed on samples previously heated up to about 600 K.

Prior to crystallization-induced shrinkage, the $Nb_{4.5}$ alloys expand more than the Nb_3 ones, as seen in Fig. 2. Otherwise, the compositional variation of maximal dilatation is rather flat except around 13 at.% Si. This concentration looks as critical also in the net shrinkage compositional variation (Fig. 3) although here the variation is not flat. Similar behavior has been observed for compositional variation of T_x from DSC measurements (see Table 1). T_x as well as the temperature of crystallization onset, almost linearly grows with x below certain x_{crit} and falls above, despite the Nb contents (also for DSC, the critical composition x_{crit} is about 13 at.% Si). However, the delay (T runs with time) in the shrinkage onset (Fig. 1) is not primarily due to the delay in attaining the crystallization onset or T_x. The incipient crystallization is seen to win the contest with expansion no sooner than it causes the average density to increase, thus making

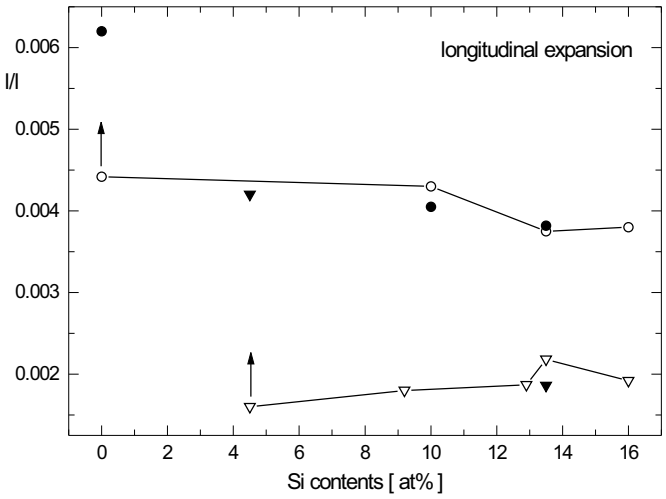

Fig. 2. Maximal dilatation $\Delta l/l$ vs. Si contents of investigated samples of Nb_3 (triangle) and $Nb_{4.5}$ (circle) heated in Ar - open symbols/ in air - full symbols. $\Delta l = l_{max} - l$; l is the length of an as-cast sample at r.t..

a sample to shrink. This is rather due to the volume percentage and density increment of the crystalline phase, than to the crystallization temperatures themselves. There is enough evidence that the compositions around 13 at.% of Si, if annealed close to their T_x (the highest T_x in the series), rapidly attain the highest crystalline share if compared to other Si percentages [10,11]. Moreover, these compositions produce the dense DO3 structure of crystalline FeSi (e.g. [10]) and show the largest density increase due to crystallization [4]. The compositional variation of these effects may well be assisted by B, which do not enter the crystalline phase and takes part in crystalline share control [2]. Still more straightforward is the effect of Nb. This component is known to hinder the crystal growth [2] and this is just what we see if comparing the expansion/shrinkage of Ar-annealed alloys with 3 and 4.5 at.% Nb respectively.

The full symbols in Fig. 2 indicate clearly that the effect of annealing ambience is really remarkable in Si-poor compositions. The effect is by far not this great if watching the net shrinkage in Fig. 3. Thus something serious must have happened prior to crystallization. Although, the overall result is actually significant: All the checked air-annealed samples are less dense than Ar-annealed ones if they contain 3 at.% of Nb, the contrary applies to the samples with 4.5 at.% of Nb. Still the more dramatic effect is reflected by magnetic properties. Just these properties helped to understand what the reason is. Complex chemical reactions (not mere oxidation) on surfaces, exposed to air and/or not cleared of adsorbed gases and moisture, promote surface crystallization and give rise to severe macroscopic heterogeneity [4, 5]. Surface-adjacent layers differ from the rest of volume by crystalline share as well as by composition. The dilatation shows that prior to ("air-supported") crystallization, the expansion is enhanced - Fig. 2. The latter effect is pronounced in Si-poor compositions only. It means that the chemistry is different here and that these reactions are not the principal booster to the crystallization - more crystalline share near

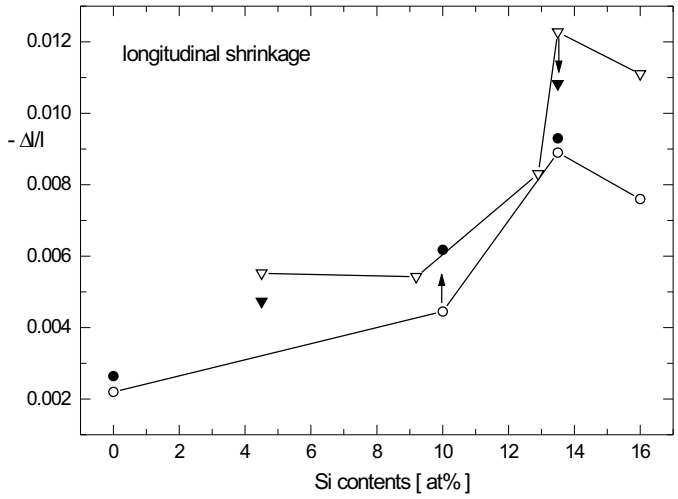

Fig. 3. Compositional variation of ultimate longitudinal shrinkage after complete temperature loop (r.t. to 900 K to r.t). Triangles stand for alloys Nb_3, circles for $Nb_{4.5}$. Open symbols stand for temperature loop in Ar ambience, full symbols for air. Δl equals final length of partially crystalline sample at r.t. minus l.

surfaces is observed at Si-rich end of the series too [12]. The other turn around, the "Si-poor processes" cannot be excluded from contributing to expel the surplus Nb to deeper layers. Then the crystal growth therein could yet be more hampered. It looks like this Nb relocation hinders the crystallization-induced shrinkage in 3 at.% Nb alloys, whereas speeding-up the surface crystallization prevails in 4.5 at.% Nb alloys.

The macroscopic heterogeneity often results in mutual bi-axial force interaction between surface layers and the volume beneath. Magnetoelastic response is then readily expected. The saturation magnetostriction λ_s of these materials decreases with greater x, until at 16 at.% Si it turns over to negative value (see Table 1). Thus except Si_{16}, the easy axis is forced off the longitudinal ribbon axis if the "volume" (assumed to be the major part of a heterogeneous sample) gets under bi-axial compression. Such an influence of the heterogeneity on the magnetic anisotropy we call the surface effect. Just this is seen in Fig. 4 for $Si_{4.5}$, where air annealing causes the loop to tilt. The tilting indicates that the major easy direction points no more along the ribbon's long axis, which is the excitation/measurement axis. Moreover, the marked "belly" at low field hints to the presence of longitudinal easy direction in a minor part of the sample. Such a loop is typical for magnetic anisotropy dominated by easy direction pointing normal to the ribbon plane with closure domains at the surfaces. Hardly resolvable effect of this kind is seen for Si_{13}. Consulting the magnetization work W_m (Table 1) is useful to see that the response to air annealing for compositions in between 0 and 13 at.% of Si lies as well in between the corresponding extremes, despite of the Nb contents. This concerns also the permeability to a lesser extent. Yet another point on the role of Nb deserves a comment. To avoid confusion with Si_{13} loops, no loop for less annealed (1 h or shorter) $Si_{4.5}$ is displayed on Fig. 4 - the loops would closely overlap. Instead, Fig. 5 presents loops for Si_0^* showing, that a Si-poor composition does not respond to prolonged

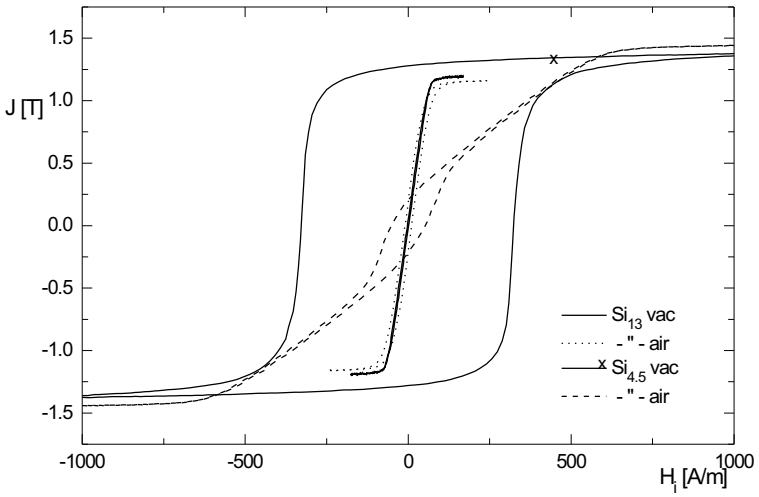

Fig. 4. The hysteresis loops of Si_{13} and $Si_{4.5}$ straight ribbons annealed at 540 °C 2h in vacuum and air, respectively.

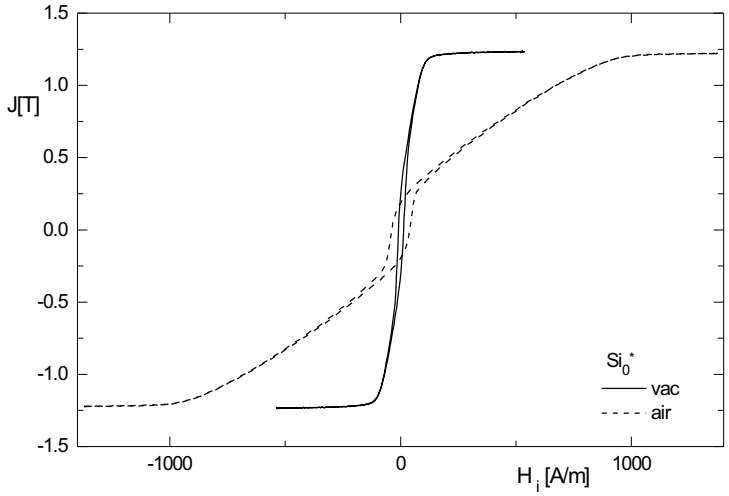

Fig. 5. The hysteresis loops of Si_0^* straight ribbons annealed at 540 °C 2 h in vacuum and air, respectively.

vacuum annealing with thick loop, if it contains enough Nb. There are two candidates to explain the thick loop: Supercritical grain size and the presence of magnetically hard borides. Even after experimental effort to resolve these effects, both of them are still in play. Nevertheless, both are expected to be hindered by more Nb. Therefore we explain the thick loop as a consequence of absent Nb enrichment, which otherwise (at air annealing) takes place within the volume of

heterogeneous samples.

4 Conclusions

Except normal thermal expansion of a metal, there are roughly two processes, which govern the initial dilatation if heating up the as-cast ribbon: (i) generally heterogeneous changes of the amorphous structure hampering the dilatation and (ii) incipient crystallization reversing the expansion to shrinkage. The expansion of an as-cast ribbon is anisotropic. The shrinkage reflects composition-dependent crystalline share, the intra-grain composition and the anisotropic expansion as well. The former two issues cause the compositions with Si between 10 and 13 at.% to show as "critical" when looking at dilatation/shrinkage compositional variation. Nb known to hinder the crystal growth causes less shrinkage and allows more dilatation. The effect of annealing ambience is especially pronounced in Si-poor compositions. The effect of chemically active surfaces is that more dilatation occurs prior to crystallization and the crystallization is macroscopically heterogeneous, being far more advanced at surfaces than within deeper layers. This effect is much weaker in Si-rich compositions pointing to another chemistry of surface reactions. On the surfaces, the crystallization-hampering effect of Nb is partially diminished by effect of air-induced changes. So the air-annealed samples with 3 at.% Nb are less dense than those annealed in Ar and the contrary applies to the samples with 4.5 at.% Nb. The observed magnetic properties agree with the interpretation [12] that the materials respond to the annealing-induced macroscopic heterogeneity with magnetoelastic anisotropy. In Si-poor air-annealed alloys, the surfaces always squeeze the volume and simultaneously hinder the crystallization therein as if repelling thitherward some Nb.

Acknowledgments The authors are indebted to Drs P. Duhaj and D. Janičkovič for casting the ribbons. B.B., P.B. and E.I. are grateful for partial support by national grant agency VEGA under grant No. 2/6065/99, so is G.V. under grant No. 2/6064/99.

References

[1] G. Herzer: *IEEE Trans. Magn.* **26** (1990) 1397

[2] G. Herzer: in *Handbook of Magnetic Materials*, ed. by K.H.J Buschow, Elsevier Science B.V., Amsterdam 1997, p. 417

[3] P. Butvin, B, Butvinová, J. Novák, G. Vlasák, P. Duhaj: *Key Engineering Materials* **81-83** (1993) 407

[4] P. Butvin, J. Sitek, B. Butvinová, E. Illeková: *J. Phys. IV* (France) **8** (1998) Pr2-123

[5] P. Butvin, B. Butvinová: *J. Electrical Engineering* **50**, 8/s (1999) 119

[6] G. Vlasák, P. Duhaj, H. Patrášová, P. Švec: *J. Phys. E: Sci.Instruments* **16** (1983) 1203

[7] D. Schermeyer, H. Neuhäuser: *Mater. Sci. Eng. A* **226-228** (1997) 846

[8] G. Vlasák, Z. Kaczkowski, P. Švec, P. Duhaj: *Mater. Sci. Eng. A* **226-228** (1997) 749

[9] P. Butvin, M. Hlásnik, G. Vlasák, B. Butvinová: *Key Engineering Materials* **40-41** (1990) 451

[10] J. Sitek, M. Miglierini, I. Tóth: *Acta Phys. Slovaca* **46** (1996) 147

[11] J. Sitek, M. Miglierini: *Acta Phys. Slovaca* **45** (1995) 21

[12] P. Butvin, B. Butvinová, Z. Frait, J. Sitek, P. Švec: *J. Magn. Mater.* **215-216** (2000) 293